

City-scale assessment of stationary energy storage supporting end-station fast charging for different bus-fleet electrification levels

Florian Trocker^a, Olaf Teichert^{a,*}, Marc Gallet^a, Aybike Ongel^a, Markus Lienkamp^{a,b}

^aTUMCREATE Ltd., 1 #10-02 Create Way, CREATE Tower, 138602 Singapore.

^bInstitute of Automotive Technology, Technical University of Munich, Garching 85748, Germany

This is the "Accepted Manuscript" version of this paper. Please see <https://doi.org/10.1016/j.est.2020.101794> to access the version of record.
(Received 23 June 2020, Revised 21 August 2020, Accepted 24 August 2020, Available online 3 September 2020)

Abstract

Fast-charging electric buses at bus end-stations can lead to high peak-demand charges for bus operators. A promising method to reduce these peak-demand charges is combining the fast charging station (FCS) with a stationary energy storage unit (SES). This work analyses the potential cost reduction for installing optimally-sized SES at bus FCS on a city scale for different levels of bus-line electrification. Results show that the cost-reduction potential reduces with increasing levels of bus-line electrification. For a case study based on the Singapore bus network, installing an SES at FCS can reduce the total costs by 1.8 % on average when 30 % of the bus lines are electrified, while the average cost reduction in a fully electrified bus network is 0.4 %. A comparison of the results with previous studies showed that the cost reduction potential is highly sensitive to the peak demand pricing method.

Keywords— stationary energy storage, peak shaving, electric public bus, city-scale simulation, optimal sizing

Nomenclature

CRF	Cost-reduction factor.	n_{max}	Maximum cycle life of the battery cell.
C_{bat}	Annual discounted depreciation of the battery costs in USD/year.	P_{bat}	Charging power of the SES in kW.
$C_{dc/dc}$	Annual discounted depreciation of the DC/DC converter costs in USD/year.	P_{cs}	Requested power from all the buses simultaneously charging at a charging station in kW.
C_{demand}	Annual demand cost in USD/year.	P_{grid}	Requested power from the grid at a charging station in kW.
C_{energy}	Annual energy cost in USD/year.	P_{lim}	Limit for the average power consumption in kW.
C_{tot}	Annual discounted depreciation of all considered costs in USD/year.	$P_{cs,\Delta t}$	Average power request at a charging station over a fixed time interval Δt in kW.
C_{tru}	Annual discounted depreciation of the transformer rectifier unit costs in USD/year.	$P_{grid,\Delta t}$	Average power request from the grid over a fixed time interval Δt in kW.
Cr_c	Maximum C-rate for battery charging in 1/h.	$\hat{p}_{month}^{\Delta t}$	Maximum value of the average power consumption within all time periods Δt in a month in kW.
Cr_d	Maximum C-rate for battery discharging in 1/h.	q	Capital recovery factor.
c_{bat}	Battery specific costs in USD/kWh.	t_{max}	Maximum shelf life of the battery cell.
$c_{dc/dc}$	Specific costs for the DC/DC converter in USD/kW.	$t_{eol,x}$	Time in years until end of life from the component $x \in \{bat, tru, dc/dc\}$ is reached.
c_{dem}	Demand price in SGD/kW.	Δt	Time interval for the calculation of peak-power average in minutes.
c_{energy}	Electricity price in SGD/kWh.		
c_{tru}	Specific costs for the transformer rectifier unit in USD/kVA.		
E_{bat}	Storage capacity in kWh.		
FEC_{day}	Number of full equivalent cycles of the battery in cycle/day.		
i	Interest rate in %.		
K	Number of time intervals Δt in a month for the calculation of the demand charges.		

Acronyms

BEB	Battery electric bus.
BLEL	Bus-line electrification level.
CRF	Cost-reduction factor.
FCS	Fast charging station.
FEL	Fleet electrification level.
SES	Stationary energy storage.
SOC	State of charge.
TRU	Transformer rectifier unit.

*This work was financially supported by the Singapore National Research Foundation under its Campus for Research Excellence And Technological Enterprise (CREATE) programme.

*Corresponding author, olaf.teichert@tum-create.edu.sg

1. Introduction

The transport sector faces numerous challenges including fossil fuel dependency, emission of local pollutants and a low energy efficiency. Electric vehicles offer a promising solution to address these challenges [1]. Public transport buses are particularly well suited for electrification, due to their fixed operating schedules and shared infrastructure [2]. Therefore, Singapore has committed to replacing 100 % of its internal combustion engine buses with electrified or hybrid buses by 2040 [3].

One major challenge for the electrification of the public bus network arises from the necessary charging infrastructure. Previous studies have shown that charging buses at route end-points, referred to as end-station charging, leads to lower operating costs, since it enables a smaller vehicle battery to be used compared with charging at the depot, and requires less charging infrastructure compared with charging at individual bus stops [4]. However, fast charging stations (FCS) at bus termini cause a high intermittent power demand, which can lead to high peak-demand electricity charges (also known as demand charges or capacity charges), or may require expensive grid reinforcements [5]. One study reported that the demand charges for a 500 kW fast charger in Tallahassee, Florida made up 75.2 ± 8.6 % of the total electricity bill [6]. Other studies investigated the required grid reinforcement and found that the impact is minor if only a small number of buses are electrified, but may increase for higher electrification levels [7, 8].

One promising method to mitigate high peak-demand charges and expensive grid reinforcements is to combine the FCS with stationary energy storage (SES) [9, 10, 11]. This enables the chargers to draw power from the SES instead of the grid during high power demand phases in order to reduce the peak load.

Numerous studies focused on optimising the configuration and operation of SES for light passenger vehicle chargers [12, 13, 14]. However, the dynamics of the charging demand of light passenger vehicles are inherently different from the charging demand created by buses, since buses operate according to a fixed schedule, resulting in a more regular charging load. Moreover, the heavy-duty operation of public buses results in higher energy requirements per trip, while the available time and locations for recharging are limited. Consequently, the charging load per charger is composed of sequences of high charging power over short charging duration, leading to significant power fluctuations when aggregated at the charging station level. Only few publications focus on the use case of supporting fast charging electric buses at end-stations.

Ding et al. (2015) optimised the battery and transformer size for an existing FCS with six 450 kW chargers in China, concluding that installing an SES can reduce the total cost by 22.85 %. The implementation of a strategy that coordinates the charging processes of the buses to reduce the total costs (coordinated charging) had only a minor impact [15].

He et al. (2019) investigated the optimal deployment of FCS for battery electric buses (BEB), minimising the total cost of vehicle batteries, chargers, SES, and electricity demand charges. The authors implemented their optimisation method for a bus

system with eight bus lines, and found that installing SES can reduce the total system cost by 9.2 % [16].

Yan et al. (2018) studied the effect of implementing an SES and coordinated charging for a single FCS in Beijing with 8 chargers. The authors used a prescient particle swarm optimisation to find the bus charging schedule that minimises the peak power and optimally uses different electricity tariffs. The battery size is optimised considering the cost for the battery, the converter and the energy cost [17]. Results showed that installing an SES can reduce the system costs by 19.1 %. In a later work, the authors investigate the optimal electric integration of the SES in the charging station [18].

Wei et al. (2020) optimised the SES configuration for catenary-free trams. Apart from a different energy-consumption profile, the basic structure of the charging system does not differ from that of a bus charging station. The authors analysed the system cost of two different methods for integrating the SES in the grid and three different SES technologies, concluding that installing a battery-based SES (with a specific battery price of 1000 EUR/kWh) can reduce costs by 1.54 % compared to an FCS without an SES [19].

Other studies investigated the feasibility of installing an SES at bus charging stations or developed energy management strategies for this use case, without optimising the size of the SES [7, 20, 21, 22].

Although previous studies have shown the benefit of battery-buffered end-station charging, the results are generally limited to a single or small number of bus termini. Few studies (e.g. [23, 24]) included the realistic modelling or analysis of the electrification of a large-scale public bus network, including the effects of sharing charging infrastructure between various bus lines. These large-scale studies, however, did not include stationary storage considerations. Moreover, the electrification of the public transport system of cities will be an ongoing process happening in stages, yet different levels of bus line electrification have not been considered in previous research.

This work evaluates the potential cost savings of installing SES at bus charging stations for end-station charging buses. A case study is conducted for the entire public bus network of Singapore at different electrification levels using FCS power demand data generated by a city-scale, agent-based simulation [25]. To find the maximum attainable cost reduction, a prescient algorithm decides when to charge and discharge the SES and the SES configuration is optimised for each bus charging station. The paper provides the following contributions:

- A novel approach to optimising configuration of an SES supporting an FCS including the impact of battery ageing.
- An in-depth analysis of the impact of the system configuration on the individual cost components, using a parameter sensitivity analysis.
- A city-scale assessment of the economic potential of installing an SES at FCS for different bus line electrification levels, based on a case study in Singapore.

The results can be used by transport planners as a reference for implementing end-station charging. The optimi-

sation algorithm and the charging demand profiles used for the case study are available open-source and can be accessed at the following repository: <https://github.com/TUMFTM/BatteryBufferedEndStationCharging>.

2. Method

The economic potential of an FCS with SES is expressed by a cost-reduction factor (CRF), given by Eq. (1), where C_{tot} denotes the annual discounted depreciation of all costs that are affected by installing an SES in USD/year and E_{bat} denotes the SES battery capacity. $C_{\text{tot}}(E_{\text{bat}} = 0)$ therefore refers to the case where no SES is installed.

$$CRF = 1 - \frac{C_{\text{tot}}}{C_{\text{tot}}(E_{\text{bat}} = 0)} \quad (1)$$

The SES supports all chargers of the charging station and is integrated behind the distribution grid transformer, connected to the direct current bus with a DC/DC converter as shown in Fig. 1. This was found to be the optimal electric integration by Yan et al. [18]. Only the cost components that are affected by installing an SES are considered, given by Eq. (2), where C_{bat} denotes the annual discounted depreciation of the battery, $C_{\text{dc/dc}}$ refers to the annual discounted depreciation of the additional DC/DC converter for the SES, C_{tru} is the annual discounted depreciation of the transformer rectifier unit, C_{energy} is the annual energy cost and C_{demand} the annual peak-demand cost.

$$C_{\text{tot}} = C_{\text{bat}} + C_{\text{dc/dc}} + C_{\text{tru}} + C_{\text{energy}} + C_{\text{demand}} \quad (2)$$

The battery cost is derived from the capacity of the SES multiplied by the specific battery cost at pack level as shown in Eq. (3). To compare the investment cost with operating costs, such as electricity cost, all investment costs are depreciated by the annual capital recovery factor q . This factor takes the lifetime of the component t_{eol} and the rate of interest i for the investment into account, as given in Eq. 4.

$$C_{\text{bat}} = E_{\text{bat}} c_{\text{bat}} q_{\text{bat}} \quad (3)$$

$$q_x = \frac{i(1+i)^{t_{\text{eol},x}}}{(1+i)^{t_{\text{eol},x}} - 1} \quad \text{for } x \in \{\text{bat, tru, dc/dc}\} \quad (4)$$

The time until the end of life of the battery $t_{\text{eol, bat}}$ is calculated with a linear ageing model that superimposes calendar and cyclic ageing, similar to [26]. First, the number of full equivalent cycles occurring on a single day is calculated using Eq. (5), where $P_{\text{bat}}(t)$ denotes the SES power. Subsequently, based on the maximum shelf life t_{max} and the maximum cycle life n_{max} of the cell, the battery life is calculated using Eq. (6). The lifetime of the TRU and the DC/DC converter are assumed to be independent of the SES operation and are therefore modelled as constants.

$$FEC_{\text{day}} = \frac{\int |P_{\text{bat}}(t)| dt}{2 E_{\text{bat}}} \quad (5)$$

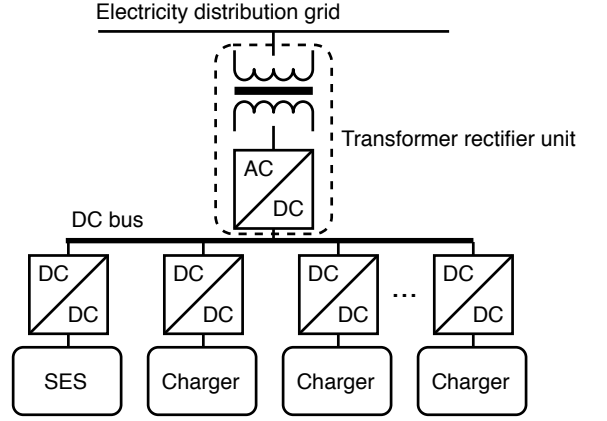


Figure 1: Integration of the SES, transformer rectifier unit, DC/DC converter and the charger in the charging station.

$$t_{\text{eol, bat}} = \frac{n_{\text{max}} t_{\text{max}}}{n_{\text{max}} + FEC_{\text{day}} t_{\text{max}}} \quad (6)$$

For the calculation of the yearly DC/DC converter cost, the converters of the chargers are not considered, because they are not influenced by installing an SES. It is assumed that the DC/DC converter for the SES will be sized according to the maximal power of the battery, calculated with the size E_{bat} and the maximal C-rate. The cost for the DC/DC converter is calculated by Eq. (7), where Cr_d denotes the maximum C-rate during discharge, Cr_c is the maximum C-rate during charging, $c_{\text{dc/dc}}$ is the specific cost in USD/kW and $q_{\text{dc/dc}}$ the capital recovery factor.

$$C_{\text{dc/dc}} = \max(Cr_d, Cr_c) E_{\text{bat}} c_{\text{dc/dc}} q_{\text{dc/dc}} \quad (7)$$

Eq. (8) gives the cost for the transformer rectifier unit, which consists of a transformer and an AC/DC converter. The cost depends on the maximum power P_{tru} that the components are designed for, the specific price c_{tru} in USD/kVA and the capital recovery factor q_{tru} .

$$C_{\text{tru}} = P_{\text{tru}} c_{\text{tru}} q_{\text{tru}} \quad (8)$$

The energy cost is calculated based on the total energy taken from the grid in one year (calculated as the integral of the power drawn from the grid $P_{\text{grid}}(t)$), multiplied by the energy price c_{energy} as given in Eq. (9).

$$C_{\text{energy}} = c_{\text{energy}} \int_0^{\text{year}} P_{\text{grid}}(t) dt \quad (9)$$

In addition to the electricity consumption cost, industrial consumers are charged with a peak-demand charge C_{demand} . The peak-demand charge is calculated based on the maximum average power demand in a prescribed measurement period of duration Δt within a month. The duration of the time period is set by the distribution grid operator. $P_{\text{grid}, \Delta t}(k)$ is defined in Eq. (10) as the average power demand for the k -th time period of duration Δt in a month. The monthly peak demand $\hat{P}_{\text{month}}^{\Delta t}$ is

defined in Eq. (11) as the maximum value of $P_{\text{grid},\Delta t}(k)$ among the K time intervals in the month. Finally, in Eq. (12) the annual peak-demand charge is calculated by multiplying the specific demand cost c_{dem} with the monthly peak demand $\hat{P}_{\text{month}}^{\Delta t}$.

$$P_{\text{grid},\Delta t}(k) = \frac{1}{\Delta t} \int_{(k-1)\Delta t}^{k\Delta t} P_{\text{grid}}(t) dt \quad (10)$$

$$\hat{P}_{\text{month}}^{\Delta t} = \max_{k \in \{1, \dots, K\}} (P_{\text{grid},\Delta t}(k)) \quad (11)$$

$$C_{\text{demand}} = \sum_{\text{month}=1}^{12} c_{\text{dem}} \hat{P}_{\text{month}}^{\Delta t} \quad (12)$$

The power drawn from the grid $P_{\text{grid}}(t)$ depends on the charging station power demand $P_{\text{cs}}(t)$ and the SES power $P_{\text{bat}}(t)$ as shown in Eq. (13). By convention, $P_{\text{bat}}(t)$ is positive when the battery charges, and negative when it discharges. For an FCS without SES $P_{\text{bat}}(t) = 0$ and $P_{\text{grid}}(t) = P_{\text{cs}}(t)$.

$$P_{\text{grid}}(t) = P_{\text{cs}}(t) + P_{\text{bat}}(t) \quad (13)$$

Given a power demand profile for the charging station $P_{\text{cs}}(t)$, the charging algorithm described in Fig. 2 calculates $P_{\text{bat}}(t)$ by deciding whether to charge or discharge the SES at every time period. Different algorithms can be used for this purpose, ranging from heuristic algorithms to stochastic algorithms that take into account the probability of more buses arriving in the current peak-shaving time period. This study uses a prescient algorithm, which assumes that the charging algorithm has full knowledge of the average charging demand of future incoming buses for each interval Δt . The algorithm therefore represents a best case scenario and gives an upper bound to the cost reduction that could be achieved by installing an SES with an FCS for any SES control algorithm.

The algorithm uses a power limit P_{lim} as a decision variable in order to cap the average grid power demand $P_{\text{grid},\Delta t}$ and thus reduce the peak-demand cost. For each time period k , the average power demand requested by the charging station $P_{\text{cs},\Delta t}(k)$ is compared with P_{lim} . If $P_{\text{cs},\Delta t}(k) > P_{\text{lim}}$, the SES supports the grid by discharging, in order to provide additional power. When the average requested power drops below the limit ($P_{\text{cs},\Delta t}(k) \leq P_{\text{lim}}$), the entire power requested by the charging station is provided from the grid and the remaining available power under the limit can be used to recharge the SES. If the energy of the SES reaches the minimum State Of Charge (SOC) level while $P_{\text{cs},\Delta t}(k) > P_{\text{lim}}$, the SES cannot discharge further and the requested power is instead taken from the grid. Furthermore, the battery power is limited by the maximum C-rate of the battery cells. If the power requested by the charging algorithm cannot be provided by the SES due to these constraints, the power difference is taken from the grid, resulting in an increase of $\hat{P}_{\text{month}}^{\Delta t}$ and therefore higher demand charges.

Given the described input parameters, E_{bat} , P_{lim} and $P_{\text{cs}}(t)$, the charging algorithm calculates $P_{\text{bat}}(t)$, $P_{\text{grid}}(t)$ and the SOC

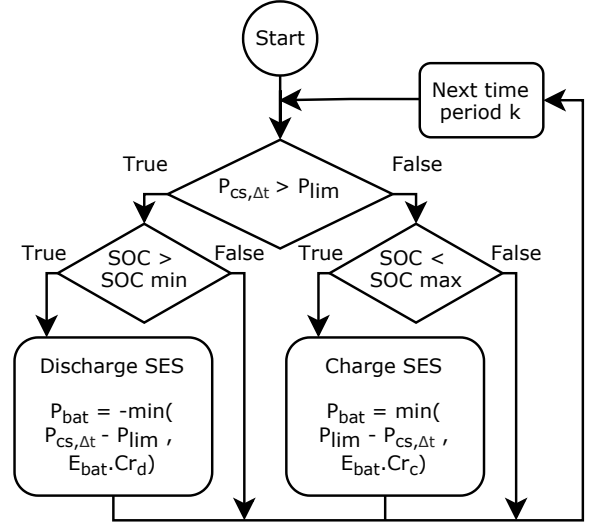


Figure 2: Flowchart of the charging algorithm.

curve as shown in Fig. 3. These curves are used to calculate C_{tot} based on Eq. (3)–(12). The optimal cost C_{tot}^* of installing an SES at a charging station is obtained by minimising C_{tot} for the two decision variables E_{bat} and P_{lim} , as given in Eq. (14).

$$C_{\text{tot}}^* = \min_{E_{\text{bat}}, P_{\text{lim}}} C_{\text{tot}}(E_{\text{bat}}, P_{\text{lim}}, P_{\text{cs}}(t)) \quad (14)$$

Using the Nelder-Mead optimisation method, new values of E_{bat} and P_{lim} are determined for each iteration until a convergence criterion is reached. If the installation of an SES at a charging station increases the total costs of the charging station, E_{bat} converges to zero and P_{lim} to the maximum of $P_{\text{cs}}(t)$. In this case, no SES is installed at the respective charging station and the CRF gives a value of zero.

3. Case study

To determine the economic potential of FCS with SES on a city-scale level, the methodology presented in Sec. 2 is applied in a case study of the public bus network in Singapore with the parametrisation shown in Table 1. In Singapore, the demand charge is calculated based on a contracted and an uncontracted price. The latter applies if the requested demand exceeds the contracted capacity and is calculated based on the averaging time interval $\Delta t = 30$ minutes [27]. At charging stations without an SES, the monthly peak demand $\hat{P}_{\text{month}}^{\Delta t}$ is considered as contracted and priced with the contracted capacity charge. For a charging station with SES, however, the contracted capacity is set to the power limit determined by the optimisation, P_{lim} . When $\hat{P}_{\text{month}}^{\Delta t}$ exceeds the power limit, the uncontracted demand charge is applied to the power demand above the contracted capacity. The energy price for the electricity is based on the annual average wholesale market price from 2019 [28].

The power demand profiles of bus charging stations are generated from city-scale simulations of the public bus system of

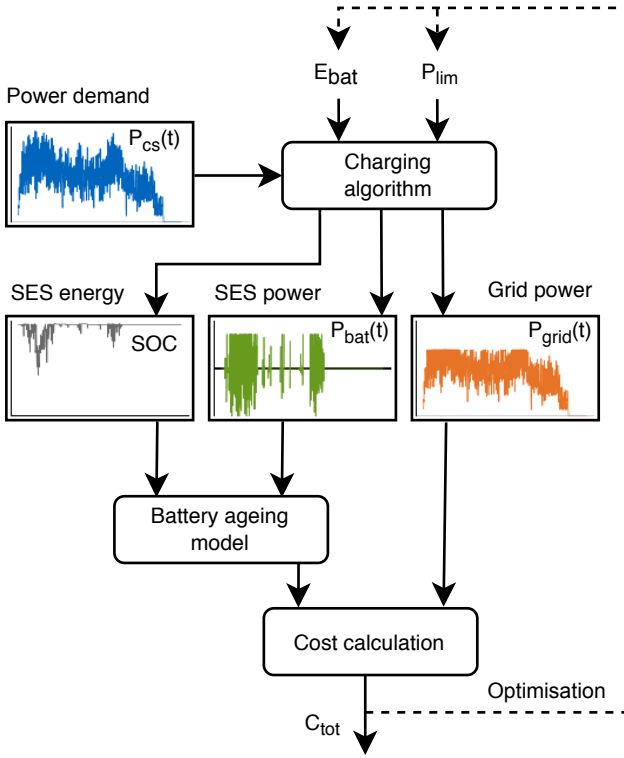


Figure 3: Methodology to optimise the total costs of a charging station based on a power demand profile.

Table 1: Constant parameters for the implementation of the case study

Parameter	Value	Unit	Source
Interest rate	5	%	[19]
Battery price (pack level)	112	USD/kWh	[29]
TRU price	11.89	USD/kVA	[18]
DC/DC converter price	74.29	USD/kW	[18]
Lifetime TRU	20	year	[18]
Lifetime DC/DC converter	8	year	[18]
Electricity price	0.0983	SGD/kWh	[28]
Contracted demand charge	8.90	SGD/kW	[27]
Uncontracted dem. charge	13.35	SGD/kW	[27]
Currency exchange rate	1.375	SGD/USD	[29]
C-rate charge	2	C	[30]
C-rate discharge	3	C	[30]
Efficiency of the SES	90	%	[31]
Min. SOC of the SES	10	%	[18]
Max. SOC of the SES	90	%	[18]
Max. calendaric life SES	15	year	[26]
Max. cycle life SES	10,000	cycle	[26]

Table 2: Bus-line electrification levels with corresponding fleet electrification level

BLEL	30 %	50 %	70 %	80 %	90 %	100 %
FEL	10 %	17 %	40 %	55 %	75 %	100 %

Singapore. Six scenarios are defined, whereby the percentage of bus lines that are fully electrified varies from 30 % to 100 %. In each scenario, the bus lines with a lower average energy demand per trip are electrified first. This leads to a non-linear relationship between the percentage of bus lines that are electrified and the percentage of the bus fleet that needs to be composed of BEB. Table 2 shows the fleet electrification levels (FEL) used in this study for the different bus-line electrification levels (BLEL).

Under the Land Transport Master Plan 2040, Singapore has committed to having a bus fleet fully powered by cleaner energy sources, consisting of electric and hybrid vehicles, by the year 2040 [3]. Therefore, the above mentioned electrification scenarios will happen within the next 20 years. As 20 years is within the lifetime of the transformer rectifier unit, this element has to be designed for the highest power within the period. For the case study in this work, the value of P_{tru} for all scenarios is therefore set independently of the electrification level by using the highest peak power determined at BLEL 100.

The power demand curves for each FCS, were generated using the City Mobility Simulator (CityMoS), an agent-based, discrete-event, traffic simulation platform under development by research teams at TUMCREATE [32, 33]. This platform is able to simulate sub-microscopic traffic with high performance on large-scale road networks. A CityMoS extension models the operation and charging behaviour of a fleet of public electric buses [25].

Bus routes in the simulation are modelled as sequences of road links between consecutive bus stops located on the road network. For service trips, bus agents follow the bus route, slowing down and stopping at each bus stop. The start or end point of each bus route is defined as a bus terminus. At the end of each service trip, the bus is parked in the terminus until the next departure. Due to the limited parking capacity in bus termini, buses are parked in bus depots while they are not in service. Off-service trips arise from bus trips between termini and depots without passengers and without following a bus route nor stopping at bus stops. When termini have a low number of available buses and upcoming departures require more buses to be dispatched (for example, before and at the beginning of peak hours), depots send buses to termini (*pull-out* trips). Conversely, when the number of buses inside termini is high (for example, at the end of peak hours) and the parking capacity of the terminus is insufficient, then buses will be put off service and drive back to depots (*pull-in* trips).

The simulated bus scenarios are based on schedules from bus lines in Singapore collected in February 2019 from the Land Transport Authority's open data portal [34]. After removing a small number of special bus lines, the remaining count of trunk and feeder bus lines is 450. Trip departure scheduling for each

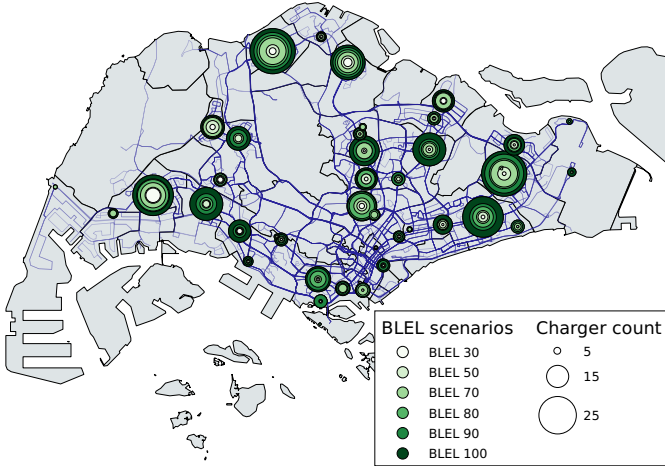


Figure 4: Map of Singapore with the location of fast-charging stations at bus termini and their respective number of chargers for each electrification scenario.

bus route is based on the average headway between two consecutive departures derived from the collected bus route data. This headway is expressed in minutes, and varies for each bus line and for different time periods of the day (before AM peak; AM peak; after AM peak; PM peak; after PM peak). The first and last departure time of each bus route is also taken from the real data set. In the simulated scenarios, the total bus fleet size was set to 6681 buses. There are 43 termini and for each scenario, five consecutive weekdays of bus operation were simulated.

The energy consumption of BEB is calculated using a longitudinal dynamics model, where the traction force to achieve a desired acceleration and speed is computed at each time step as a function of the air drag, rolling resistance, road inclination and inertial force. The mechanical power for the traction force is provided by an electric powertrain chain, including efficiencies of the transmission gearbox, the electric motor and the inverter drawing power from the bus battery. The tractive force can be negative, for example while braking or driving on a downward slope. In that case, some of the energy can be recuperated and used to recharge the battery. In addition, the energy demand for air-conditioning is computed based on the time of day and passenger occupancy.

After a trip, electric buses opportunistically recharge at charging stations located in the bus termini and depots. In the studied scenarios, these charging stations are equipped with fast chargers with a nominal power per charging point of 450 kW. For each electrification scenario, the number of chargers installed at each charging station was set such that each charger has a minimum utilisation factor of 10% and each charging station has at least two chargers. Fig. 4 shows how the number of chargers increases with the BLEL at the FCS locations.

If a BEB has less than 80% SOC after a trip, it attempts to recharge immediately provided that a charger is available. Otherwise it is placed in a waiting queue for charging. Once the bus is sufficiently recharged, it leaves the charger and parks in the bus terminus or depot until the next trip departure. After a charger becomes available again, a bus from the waiting queue (if any) is selected for charging. To model the time needed for

Table 3: Comparison of the yearly cost from the charging station at Kent Ridge Terminal for BLEL = 50%, with and without optimal SES

	Charging station without SES	Charging station with opt. SES	Unit
P_{lim}	-	238	kW
E_{bat}	-	98	kWh
$T_{eol, bat}$	-	10.9	year
C_{bat}	-	1338	USD/year
$C_{dc/dc}$	-	3409	USD/year
C_{tru}	2524	2470	USD/year
C_{energy}	69,443	69,622	USD/year
C_{demand}	25,150	18,507	USD/year
C_{tot}	97,117	95,346	USD/year

the previous bus to vacate the charging point and for the next bus to take its place, the simulation imposes a delay of 2 min between consecutive charging events at the same charger.

The total power demand of each charging station is computed by summing up the instantaneous charging power of each of its chargers, and is stored every 10 seconds. This results in 6 charging curves (one for each scenario) for each charging station at a terminus over five consecutive days of bus operation. These power curves are used as input for the power demand $P_{cs}(t)$ defined in Sec. 2.

4. Results

To illustrate the charging algorithm and the cost calculations, the details for a single bus terminus and scenario are shown first in Sec. 4.1. Subsequently in Sec. 4.2, the trade-offs involved in the optimisation are shown with a parameter sensitivity study. Finally, the potential cost reduction of installing an SES at an FCS for all charging stations in each scenario is presented in Sec. 4.3.

4.1. Peak shaving and cost reduction for a single charging station

To illustrate the SES optimisation, the detailed results of the charging station located at the *Kent Ridge Terminal* are presented for the electrification scenario BLEL = 50%. The costs of an FCS with an optimal-sized SES and without an SES are compared in Table 3.

The total annual costs of the charging station can be reduced from 97,117 USD/year to 95,346 USD/year (CRF = 1.8%) with an optimal-sized SES. The energy costs in both configurations account for more than 71% of the total costs. For the charging station without SES, the demand costs make up 25.9% of the total costs, while installing an SES reduces the share of demand costs to 19.4% of the total costs. The battery cost increases the total costs by 1.4%.

Fig. 5 shows the operation of the fast charger and the SES over the simulated period of five days. The top graph displays the power demand curve along with the 30-minute average. The resulting power curves for the grid and battery along with the

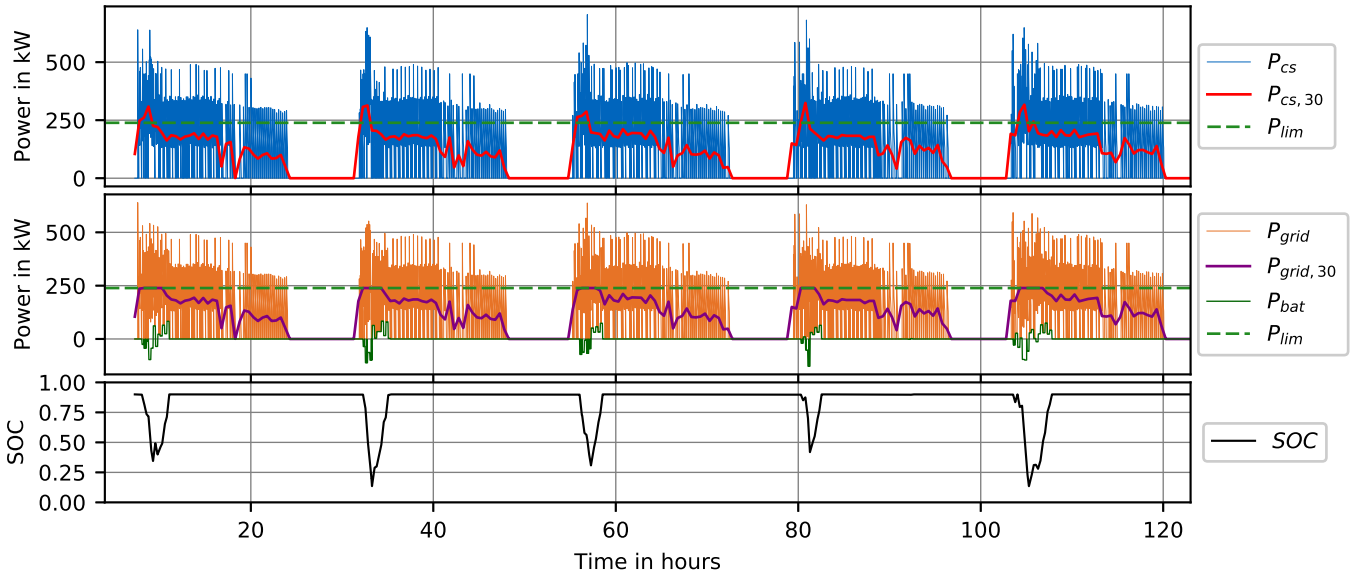


Figure 5: Power curves and SOC of the SES of the charging station at *Kent Ridge Terminal* for BLEL = 50 %

30-minute average of the grid power are shown in the middle graph. A negative value for the battery power indicates that the SES is discharged to mitigate the peaks in the power demand curve. The SES successfully lowers the peak-demand charge by supporting the grid at times when the 30-minutes average power demand would exceed the power limit. The bottom graph shows the corresponding SOC curve of the SES. The daily differences in the minimum SOC stem from the daily differences in the charging power curve $P_{cs}(t)$. These differences are caused by the road traffic simulation, which considers stochastic delays that affect the trip duration and arrival time of buses at end-stations.

4.2. Parameter sensitivity analysis

A sensitivity analysis is conducted to assess the impact of the SES capacity and the power limit on the different costs as shown in Fig. 6. The orange dot marks the optimum configuration of the SES. The orange line divides the plot between configurations that exceed the power limit (bottom left) and configurations that do not exceed it (upper right). All costs are normalised to the total cost at the optimal configuration, C^* .

The demand costs, C_{demand} , decrease with the reduction of the power limit, if the latter is not exceeded, as shown in Fig. 6a. For low power limits with small SES, the minimum SOC is reached and P_{lim} is exceeded. The requested power P_{cs} is charged from the grid and thus the demand costs below the line increase. Decreasing the battery size and power limit further causes the power limit to be exceeded more frequently, thereby increasing costs.

The energy cost increases for lower power limits, as shown in Fig. 6b. A lower power limit leads to a higher utilisation of the SES and, due to the efficiency losses while charging and discharging the SES, leads to a higher energy consumption.

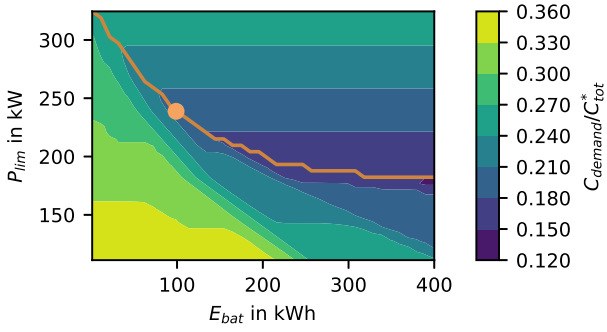
The cost for the SES increases with the capacity of the SES, as shown in Fig. 6c. Additionally, the implications of battery ageing, calculated by eq. 3-6, can be seen. When the power limit is lowered for a given SES capacity, the energy throughput increases, increasing the number of full equivalent cycles. The increase in full equivalent cycles reduces the battery life and therefore increases the annual depreciation of the battery costs. This relationship holds true for configurations where the SES is not fully discharged, i.e. above the orange line in Fig. 6c. For fully discharged configurations the energy throughput does not uniformly increase further for lower power limits.

Fig. 6d shows the total costs, depending on the capacity of the SES and the power limit, for the selected charging station and scenario. The dot lies above the line, indicating that the limit is not exceeded at this terminus with the optimal configuration of the SES.

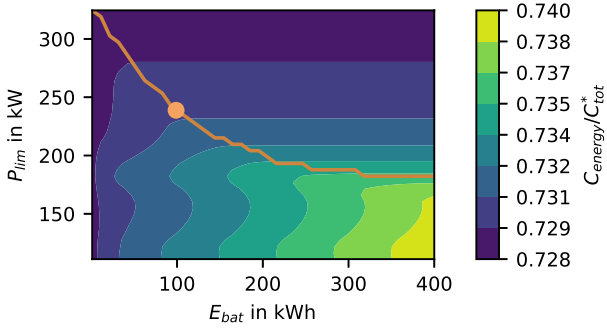
4.3. Cost reduction of all charging stations under different scenarios

The economic potential of installing an FCS with SES was analysed for 43 charging stations at bus termini under six electrification levels. An Analysis of Variance (ANOVA) was conducted and showed that the BLEL has a significant impact on the CRF ($F < p$; $F = 9 \times 10^{-6}$; $p = 0.05$).

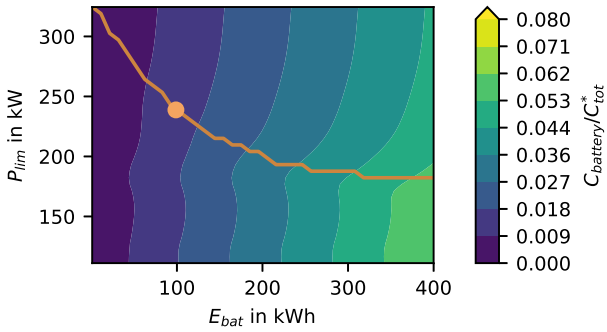
Fig. 7 shows the distribution of the CRF for all charging stations grouped by the different BLEL. The horizontal line inside the boxes refers to the median, the cross (X) sign shows the mean and the whiskers are set at the 5th and the 95th percentile. The figure shows that the mean and median CRF decrease with increasing BLEL. At BLEL 30, The CRF ranges from 0.1 % to 11.7 % with a mean of 1.8 %, while for a fully electrified bus network (BLEL 100), the CRF ranges from 0 % to 1.6 % with a mean of 0.4 %.



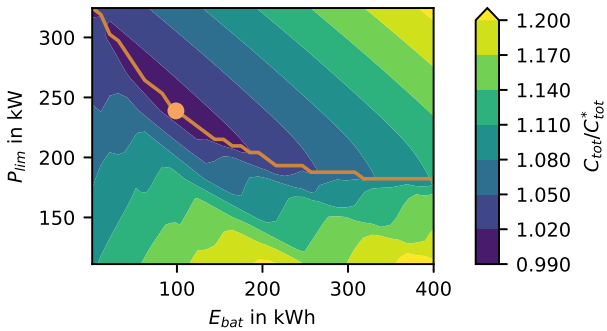
(a)



(b)



(c)



(d)

Figure 6: Contour plots of (a) demand costs, (b) energy costs, (c) battery costs and (d) total costs with the optimal configuration of the SES at *Kent Ridge Terminal* for BLEL = 50 %

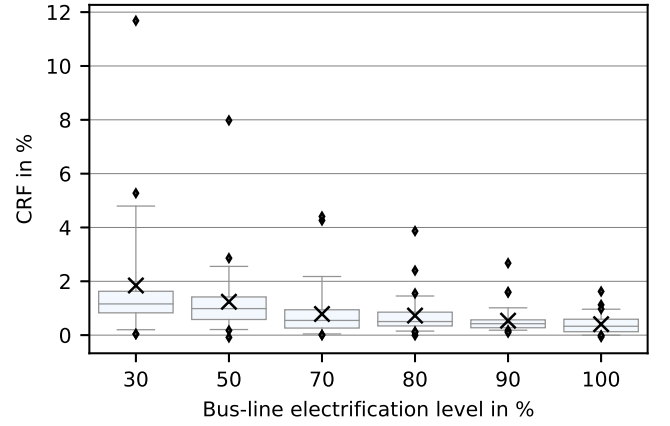


Figure 7: Distributions of the CRF of 43 charging stations for 6 electrification scenarios. (Box plot whiskers set at 5th and 95th percentile)

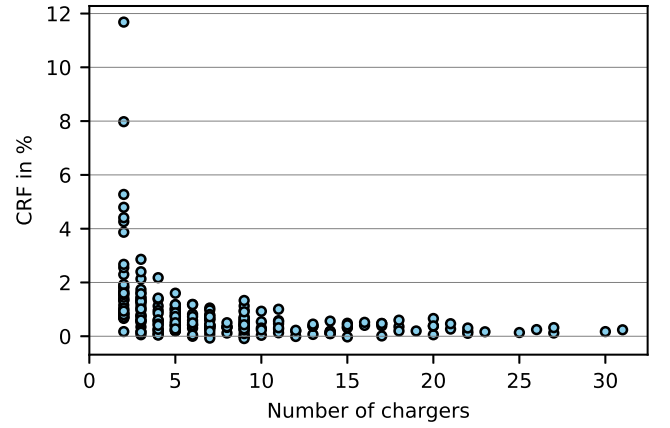


Figure 8: Distribution of the CRF depending on the number of chargers per charging station for all charging stations and electrification scenarios

To explain the variation of the CRF within BLEL scenarios, Fig. 8 shows the CRF for all charging stations in all scenarios as a function of the number of chargers at an FCS. The number of chargers at an FCS for a given BLEL is determined by the charger placement method and varies among termini, as shown in Fig. 4. The highest CRF values occur at termini with few chargers, since fewer bus lines end at these termini, leading to a more sporadic charging demand and higher share of demand costs in the total costs.

The effectiveness of reducing the peak-demand charges by installing an SES is illustrated in Fig. 9. For charging stations without SES, it can be seen that the share of demand costs decreases with increasing BLEL. This is explained by the increase in total energy consumption of the bus fleet, which causes the energy costs, C_{energy} , to increase at a greater rate than the demand costs, C_{demand} , thus reducing the share of the latter in the total costs. Consequently, the potential to reduce demand costs is more limited at higher electrification levels, which explains the lower CRF at higher BLEL seen in Fig. 7. At the lowest BLEL considered in this work, the demand costs account for 16.1 % to 47.2 % of the total costs. With optimal sized SES,

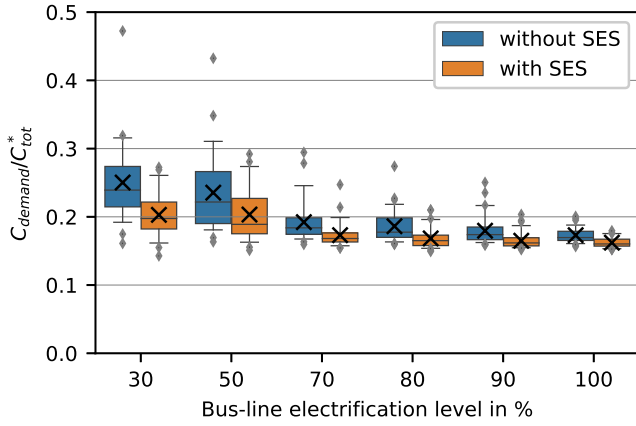


Figure 9: Distributions of the share of the demand costs within the total costs with and without optimal SES for each electrification scenario. (Box plot whiskers set at 5th and 95th percentile)

they decrease to less than 27.3 % for all charging stations. In the fully electrified bus network of Singapore, the demand costs account between 15.6 % and 20.0 % of the total costs without SES and can be reduced to less than 17.9 % by installing SES.

5. Discussion

Previous studies that investigated the installation of SES at bus FCS reported CRF values of 1.58 % [19], 9.2 % [16], 19.1 % [17] and 22.85 % [15] in case studies with few chargers per charging station, which corresponds to low BLEL. The low CRF of 1.58 % reported by Wei et al. can be explained by the use of a battery specific cost of 1000 EUR/kWh, which is an order of magnitude larger than the battery specific cost used in this study, see Table 1. The CRF of the remaining studies are higher than those obtained in this study at BLEL 30, which range from 0.1 % to 11.7 %.

One factor that contributes to the difference in results is the time interval used for calculating the average peak power demand. While utilities in Singapore use a 30-minute time window to calculate peak-demand charges, previous literature investigated bus networks where peak-demand charges were either based on a 15-minute time window, resulting in a CRF of 9.2 % [16], or on the maximum instantaneous power demand, resulting in a CRF of 19.1 % and 22.85 % [15, 17].

To highlight the impact of Δt on the CRF, the optimisation presented in this work is repeated for all FCS and BLEL using a Δt of 15 minutes. The resulting CRF values are compared with the previous results in Figure 10. For every BLEL scenario, the CRF distributions calculated with the shorter time window are higher. At BLEL 30 and $\Delta t = 15$ minutes the CRF ranges from 0.8 % to 14.4 %, which is in line with the value found by [16] for the same time window.

With a reduction of the averaging time window, the impact of short-term power peaks on the peak-demand charge increases, leading to higher demand costs when no SES is installed at the charging station. This increases the potential cost reduction that

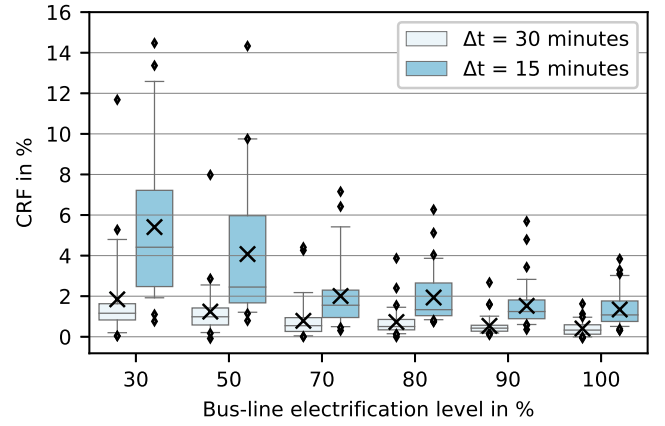


Figure 10: Distributions of the CRF of 43 charging stations for 6 electrification scenarios, for $\Delta t = 30$ minutes and 15 minutes. (Box plot whiskers set at 5th and 95th percentile)

can be achieved with an SES, resulting in higher CRF. Calculating peak demand charges based on the maximum instantaneous power consequently results in the highest cost saving potential. This shows that the pricing scheme used for peak-demand charges has a large impact on the economic potential of installing an SES with FCS.

The methodologies and the open-sourced code of this study can be used to plan and calculate the economic potential of FCS with SES in other settings. However, the following limitations of the method should be considered. First, the current implementation of the method does not limit the battery size to discrete values. This means that the cost-optimal configuration of the SES might not be available on the market, and a customisation of the size might lead to increased battery costs. Furthermore, the method evaluated the cost-reduction potential for each BLEL separately (except for the dimensioning of the transformer and AC/DC converter). When planning the construction of FCS with SES, the potential increase of the electrification level over the lifetime of the SES should be taken into account. While a change in the SES size during the lifetime introduces new costs, the power limit of the charging algorithm can be adjusted as a software parameter to reflect new operating conditions.

The presented method provides a range of opportunities for future work. First, the method can be extended to investigate the use of different storage technologies (e.g. supercapacitors), bus networks (e.g. from other cities), energy sources (e.g. photovoltaic) and other charging strategies (e.g. overnight charging). Second, the method may be used to analyse the benefit of more advanced charging algorithms for the SES, that for example take the electricity price at the time of use into account. Finally, when assuming flexible timing of the bus charging process, the use of coordinated charging to reduce or extend the opportunities of an SES could be investigated.

6. Conclusion

This work evaluated the economic benefits of combining fast-charging stations at bus termini with an SES. A methodology to minimise the costs of an SES for FCS was developed and implemented for a city-scale case study, analysing 43 charging stations at bus termini under 6 electrification level scenarios, modelling the gradual electrification of 450 Singapore bus lines.

The case study showed that the share of demand charges in the total costs of an FCS without an SES decreases with an increase in bus-line electrification. As a result, the potential cost reduction that can be achieved by installing an SES is higher for low levels of bus-line electrification. The share of the demand charges in the total cost of an FCS without SES may serve transport operators as an indicator to decide if and where to install SES.

Furthermore, a comparison with results from previous studies showed that the economic potential of installing an SES at FCS is highly sensitive to the averaging duration Δt used for calculating the monthly peak power demand. Therefore, the attractiveness of installing SES with FCS depends on the billing method used by the local grid operator to calculate demand charges.

Author contributions

Florian Trocker developed the described method and revised the paper to its final form. Olaf Teichert is the initiator of the research topic, supported the development of the method, wrote the introduction and contributed to other sections of the paper. Marc Gallet developed the model for electric public buses in the agent-based, city-scale simulation, wrote the corresponding sections of the paper and contributed to the discussion of the results. Dr. Aybike Ongel is the principal investigator of the research project and provided constructive comments on the paper. Prof. M. Lienkamp made an essential contribution to the conception of the research project. He revised this article critically for important intellectual content. Prof. M. Lienkamp gave final approval of the version to be published and agrees to all aspects of the work. As a guarantor, he accepts responsibility for the overall integrity of this article.

References

- [1] M. A. Delucchi, C. Yang, A. F. Burke, J. M. Ogden, K. Kurani, J. Kessler, and D. Sperling, "An assessment of electric vehicles: technology, infrastructure requirements, greenhouse-gas emissions, petroleum use, material use, lifetime cost, consumer acceptance and policy initiatives," *Philosophical transactions. Series A, Mathematical, physical, and engineering sciences*, vol. 372, no. 2006, p. 20120325, 2014.
- [2] M. Mahmoud, R. Garnett, M. Ferguson, and P. Kanaroglou, "Electric buses: A review of alternative powertrains," *Renewable and Sustainable Energy Reviews*, vol. 62, pp. 673–684, 2016.
- [3] Land Transport Authority, "2040 land transport master plan," Singapore, 2019. [Online]. Available: https://www.lta.gov.sg/content/ltagov/en/who_we_are/our_work/land_transport_master_plan_2040.html
- [4] A. Lajunen, "Lifecycle costs and charging requirements of electric buses with different charging methods," *Journal of Cleaner Production*, vol. 172, pp. 56–67, 2018.
- [5] M. Rogge, S. Wollny, and D. Sauer, "Fast charging battery buses for the electrification of urban public transport—a feasibility study focusing on charging infrastructure and energy storage requirements," *Energies*, vol. 8, no. 5, pp. 4587–4606, 2015.
- [6] N. Qin, A. Gusrialdi, R. P. Brooker, T. Ali, *et al.*, "Numerical analysis of electric bus fast charging strategies for demand charge reduction," *Transportation Research Part A: Policy and Practice*, vol. 94, pp. 386–396, 2016.
- [7] D. Steen and A. Le Tuan, "Impacts of fast charging of electric buses on electrical distribution systems," *CIREC - Open Access Proceedings Journal*, vol. 2017, no. 1, pp. 2350–2353, 2017.
- [8] K. Zagrajek, J. Paska, M. Kłos, K. Pawlak, P. Marchel, M. Bartecka, Ł. Michalski, and P. Terlikowski, "Impact of electric bus charging on distribution substation and local grid in warsaw," *Energies*, vol. 13, no. 5, p. 1210, 2020.
- [9] J.-B. Gallo, T. Bloch-Rubin, and J. Tomić, "Peak demand charges and electric transit buses," U.S. Department of Transportation Federal Transit Administration, Tech. Rep., 2014. [Online]. Available: <https://calstart.org/wp-content/uploads/2018/10/Peak-Demand-Charges-and-Electric-Transit-Buses.pdf>
- [10] O. Olsson, A. Grauers, and S. Pettersson, "Method to analyze cost effectiveness of different electric bus systems," in *EVS 2016 - 29th International Electric Vehicle Symposium*, 2016, pp. 604–615, conference code: 125226.
- [11] M. Andersson, "Energy storage solutions for electric bus fast charging stations : Cost optimization of grid connection and grid reinforcements," 2017.
- [12] L. Yang and H. Ribberink, "Investigation of the potential to improve dc fast charging station economics by integrating photovoltaic power generation and/or local battery energy storage system," *Energy*, vol. 167, pp. 246–259, 2019.
- [13] T. S. Bryden, G. Hilton, B. Dimitrov, C. P. de León, and A. Cruden, "Rating a stationary energy storage system within a fast electric vehicle charging station considering user waiting times," *IEEE Transactions on Transportation Electrification*, vol. 5, no. 4, pp. 879–889, 2019.
- [14] M. Aziz, T. Oda, and M. Ito, "Battery-assisted charging system for simultaneous charging of electric vehicles," *Energy*, vol. 100, pp. 82–90, 2016.
- [15] H. Ding, Z. Hu, and Y. Song, "Value of the energy storage system in an electric bus fast charging station," *Applied Energy*, vol. 157, pp. 630–639, 2015.
- [16] Y. He, Z. Song, and Z. Liu, "Fast-charging station deployment for battery electric bus systems considering electricity demand charges," *Sustainable Cities and Society*, vol. 48, p. 101530, July 2019.
- [17] Y. Yan, J. Jiang, W. Zhang, M. Huang, Q. Chen, and H. Wang, "Research on power demand suppression based on charging optimization and bess configuration for fast-charging stations in beijing," *Applied Sciences*, vol. 8, no. 8, p. 1212, 2018.
- [18] Y. Yan, H. Wang, J. Jiang, W. Zhang, Y. Bao, and M. Huang, "Research on configuration methods of battery energy storage system for pure electric bus fast charging station," *Energies*, vol. 12, no. 3, p. 558, 2019.
- [19] S. Wei, J. Jiang, N. Murgovski, J. Sjöberg, W. Zhang, C. Zhang, and X. Hu, "Optimisation of a catenary-free tramline equipped with stationary energy storage systems," *IEEE Transactions on Vehicular Technology*, vol. 69, no. 3, pp. 2449–2462, 2020.
- [20] D. Kucevic, C. N. Truong, A. Jossen, and H. C. Hesse, "Lithium-ion battery storage design for buffering fast charging stations for battery electric vehicles and electric buses," in *NEIS 2018*, D. Schulz, Ed. Berlin: VDE VERLAG GMBH, 2019, pp. 150–155.
- [21] H. Chen, Z. Hu, H. Zhang, and H. Luo, "Coordinated charging and discharging strategies for plug-in electric bus fast charging station with energy storage system," *IET Generation, Transmission & Distribution*, vol. 12, no. 9, pp. 2019–2028, 2018.
- [22] Y. Liu and H. Liang, "A root approach for stochastic energy management in electric bus transit center with pv and ess," in *2019 IEEE Global Communications Conference (GLOBECOM)*. IEEE, 2019, pp. 1–6.
- [23] M. Xylia, S. Leduc, P. Patrizio, F. Kraxner, and S. Silveira, "Locating charging infrastructure for electric buses in Stockholm," *Transportation Research Part C: Emerging Technologies*, vol. 78, pp. 183–200, May 2017.
- [24] G. Wang, X. Xie, F. Zhang, Y. Liu, and D. Zhang, "bCharge: Data-Driven

- Real-Time Charging Scheduling for Large-Scale Electric Bus Fleets,” in *2018 IEEE Real-Time Systems Symposium (RTSS)*. Nashville, TN: IEEE, Dec. 2018, pp. 45–55.
- [25] M. Gallet, T. Massier, and D. Zehe, “Developing a large-scale microscopic model of electric public bus operation and charging,” in *Proceedings of the 2019 IEEE Vehicle Power and Propulsion Conference (VPPC)*. IEEE, Oct. 2019, pp. 1–5.
- [26] H. Hesse, R. Martins, P. Musilek, M. Naumann, C. Truong, and A. Jossen, “Economic optimization of component sizing for residential battery storage systems,” *Energies*, vol. 10, no. 7, p. 835, 2017.
- [27] SP Group, “Transmission service rate schedule,” 2019. [Online]. Available: www.spgroup.com.sg/wcm/connect/spgrp/dd1fd96d-0c21-4e88-8ded-210ceb61ca3a/\%5BInfo\%5D+Transmission+Service+Rate+Schedule.pdf?MOD=AJPERES
- [28] Energy Market Company, “Uniform singapore energy price,” 2020. [Online]. Available: www.emcsg.com/marketdata/priceinformation
- [29] M. Fries, M. Kerler, S. Rohr, M. Sinning, S. Schickram, M. Lienkamp, R. Kochhan, S. Fuchs, B. Reuter, P. Burda, and S. Matz, “An overview of costs for vehicle components, fuels, greenhouse gas emissions and total cost of ownership update 2017,” Institute of Automotive Technology, Technical University of Munich, Tech. Rep., 08 2017.
- [30] 2012 SANYO Energy (U.S.A.), “Datasheet panasonic sanyo ur18650e,” 2020. [Online]. Available: <https://datasheetspdf.com/datasheet/UR18650E.html>
- [31] P. Chlebis, M. Tvrdon, A. Havel, and K. Baresova, “Comparison of standard and fast charging methods for electric vehicles,” *Advances in Electrical and Electronic Engineering*, vol. 12, no. 2, 2014.
- [32] D. Zehe, A. Knoll, S. Nair, and D. Eckhoff, “Towards CityMoS: A Coupled City-Scale Mobility Simulation Framework,” in *5th GI/ITG KuVS Fachgespräch Inter-Vehicle Communication*, ser. Technical Reports / Department Informatik, vol. CS-2017-03. Friedrich-Alexander-Universität Erlangen-Nürnberg (FAU), May 2017, p. 26.
- [33] P. Andelfinger, Y. Xu, W. Cai, D. Eckhoff, and A. Knoll, “Fast-Forwarding Agent States to Accelerate Microscopic Traffic Simulations,” in *Proceedings of the 2018 ACM SIGSIM Conference on Principles of Advanced Discrete Simulation - SIGSIM-PADS '18*. Rome, Italy: ACM Press, 2018, pp. 113–124.
- [34] Land Transport Authority, “LTA DataMall.” [Online]. Available: <https://www.mytransport.sg/content/mytransport/home/dataMall.html>